Published in final edited form as:
J Refract Surg. 2010 March ; 26(3): 183–190. doi:10.3928/1081597X-20100224-04.

Contribution of Optical Zone Decentration and Pupil Dilation on the Change of Optical Quality After Myopic Photorefractive Keratectomy in a Cat Model

Jens Bühren, MD[1,2], **Geunyoung Yoon, PhD**[1,3], **Scott MacRae, MD**[1,3], and **Krystel Huxlin, PhD**[1,3]

[1] University of Rochester Eye Institute, University of Rochester Medical Center, Rochester, NY

[2] Department of Ophthalmology, Goethe-Universität Frankfurt, Frankfurt am Main, Germany

[3] Center for Visual Science, University of Rochester, Rochester, NY

Abstract

PURPOSE—To simulate the simultaneous contribution of optical zone decentration and pupil dilation on retinal image quality using wavefront error data from a myopic photorefractive keratectomy (PRK) cat model.

METHODS—Wavefront error differences were obtained from five cat eyes 19±7 weeks (range: 12 to 24 weeks) after spherical myopic PRK for −6.00 diopters (D) (three eyes) and −10.00 D (two eyes). A computer model was used to simulate decentration of a 6-mm sub-aperture relative to the measured wavefront error difference. Changes in image quality (visual Strehl ratio based on the optical transfer function [VSOTF]) were computed for simulated decentrations from 0 to 1500 μm over pupil diameters of 3.5 to 6.0 mm in 0.5-mm steps. For each eye, a bivariate regression model was applied to calculate the simultaneous contribution of pupil dilation and decentration on the pre- to postoperative change of the log VSOTF.

RESULTS—Pupil diameter and decentration explained up to 95% of the variance of VSOTF change (adjusted R^2=0.95). Pupil diameter had a higher impact on VSOTF (median β=−0.88, P<.001) than decentration (median β= −0.45, P<.001). If decentration-induced lower order aberrations were corrected, the impact of decentration further decreased (β= −0.26) compared to the influence of pupil dilation (β= −0.95).

CONCLUSIONS—Both pupil dilation and decentration of the optical zone affected the change of retinal image quality (VSOTF) after myopic PRK with decentration exerting a lower impact on VSOTF change. Thus, under physiological conditions pupil dilation is likely to have more effect on VSOTF change after PRK than optical zone decentration.

Correspondence: Jens Bühren, MD, Dept of Ophthalmology, Goethe-Universität Frankfurt, Theodor-Stern-Kai 7, D-60590 Frankfurt am Main, Germany. Tel: 49 69 6301 6588; Fax: 49 69 6301 3893; buehren@em.uni-frankfurt.de.

Drs Yoon and MacRae are scientific consultants to Bausch & Lomb, Rochester, NY. The remaining authors have no proprietary interest in the materials presented herein.

Presented as an E-Poster at the International Society of Refractive Surgery of the American Academy of Ophthalmology Refractive Surgery Subspecialty Day; November 7–8, 2008; Atlanta, Ga.

AUTHOR CONTRIBUTIONS

Study concept and design (J.B., G.Y., S.M., K.H.); data collection (J.B., G.Y., S.M.); analysis and interpretation of data (J.B., G.Y., S.M.); drafting of the manuscript (J.B., G.Y., S.M.); critical revision of the manuscript (J.B., G.Y., S.M., K.H.); obtained funding (J.B., K.H.); administrative, technical, or material support (S.M., K.H.); supervision (S.M., K.H.)

While decreasing the amount of lower order aberrations (LOA), laser refractive surgery increases the amount of higher order aberrations (HOA)—mainly coma and spherical aberration—in the eye.[1,2] Although overall HOA induction has been shown to be lower in wavefront-guided LASIK, inherent induction of coma and spherical aberration remained.[3,4] The fact that keratorefractive surgery induces HOA has been known for a long time; however, the origin of the HOA induction remains somewhat unclear. There is evidence for a variety of causes such as loss of laser energy efficiency in the corneal periphery,[5,6] the diameter of the optical zone relative to pupil diameter,[7] random decentrations of the optical zone,[8–11] biomechanical effects,[12–14] flap-induced aberrations in LASIK,[15–17] and wound healing reactions after photorefractive keratectomy (PRK).[14,18] By applying a multivariate statistical analysis, we have shown that in uneventful wavefront-guided LASIK, the induction of spherical aberration was correlated with the amount of attempted correction and the optical zone diameter. In contrast, the induction of coma occurred in an apparently random fashion, independent from other factors.[4] These results strongly suggest that coma induction could be attributed to subclinical decentrations of the optical zone ("micro-decentrations," ie, decentrations ≤500 μm) as it has been shown that micro-decentrations are ubiquitous, random errors.[8–11]

However, the clinical impact of decentrations ≤500 μm on optical quality is still poorly understood. We recently established a computer simulation model that allows for systematic investigation of decentration effects on optical quality as well as on LOA and HOA, using real postoperative PRK wavefront data obtained from a cat PRK model.[19] Our results using this model showed a decrease in retinal image quality and induction of astigmatism, coma, and undercorrection of defocus. The study further showed that decentration tolerance was higher for a 3.5-mm than for a 6-mm pupil diameter. The latter finding prompted the following questions: how do optical zone decentration and pupil diameter interact and how does this interaction affect changes of optical quality induced by laser refractive surgery? The present simulation study was conducted to test the hypotheses that 1) optical zone decentration and pupil dilation both decrease optical quality after myopic PRK, and 2) decentrations ≤500 μm (referred to as micro-decentrations hereafter) are likely the main cause of night vision disturbances due to a steeper decrease of optical quality in eyes with micro-decentrations when the pupil dilates.

Using our cat PRK-based decentration model, we determined the change in optical quality, represented by the metric visual Strehl ratio based on the optical transfer function (VSOTF) [20] in three simulation experiments. In the first simulation, the effects of pupil dilation and optical zone decentration were investigated relative to an optimum outcome for a 3-mm pupil diameter. The second simulation examined the effects of pupil dilation and optical zone decentration relative to best-corrected image quality for a 3-mm pupil adjusted for each decentered position. This simulation represents the clinical situation of spectacle correction obtained at 3-mm pupil diameter in an eye with optical zone decentration. The third simulation assessed the effects of pupil dilation and decentration on best-corrected image quality (optimum LOA correction for each pupil diameter at each decentered position).

MATERIALS AND METHODS

Subjects and PRK Surgery

Data were obtained from five eyes of five normal male domestic short hair cats (*Felis cattus*) that underwent myopic PRK with an uncomplicated follow-up of at least 3 months and for which wavefront aberrations could be measured over a pupil diameter of 9 mm. Procedures were conducted according to the guidelines of the University of Rochester Committee on Animal Research (UCAR), the Association for Research in Vision and Ophthalmology

(ARVO) Statement for the Use of Animals in Ophthalmic and Vision Research, and the National Institutes of Health (NIH) Guide for the Care and Use of Laboratory Animals.

Three cat eyes underwent PRK for −6.00 diopters (D)—two with a programmed optical zone of 6 mm and one with an 8-mm optical zone—and two eyes received PRK for −10.00 D (6-mm optical zone). The procedure has been described in detail elsewhere.[14] Briefly, all eyes received conventional spherical ablation (Planoscan 4.14; Bausch & Lomb, Rochester, NY) performed by one of two surgeons (J.B. or S.M.) under surgical anesthesia using a Technolas 217 laser (Bausch & Lomb). The ablation was centered to the pupil, which was constricted with two drops of pilocarpine 3% (Bausch & Lomb). After surgery, the cats received two drops of 0.3% tobramycin and 0.1% dexamethasone (TobraDex; Alcon Laboratories Inc, Ft Worth, Tex) per eye once per day until the surface epithelium healed.

Wavefront Sensing and Computer Simulation of Optical Zone Decentration

As described previously,[14,21] cats were trained to fixate on single spots of light presented on a computer monitor. Wavefront measurements were performed preoperatively and 19±7 weeks (range: 12 to 24 weeks) postoperatively with a custom-built Hartmann-Shack wavefront sensor. The wavefront sensor was aligned to the visual axis of one eye while the other eye fixated on a spot on the computer monitor.[21] At least 10 measurements were collected per imaging session per eye. The simulation procedure has been described in detail in a previous publication.[19] Briefly, wavefront errors were calculated using a 2nd to 10th order Zernike polynomial expansion according to the Visual Science and its Application (VSIA) standards for reporting aberration data of the eye.[22] Centered post- to preoperative wavefront error differences $\Delta W(x, y)$ over a 9-mm pupil diameter were obtained by shifting the analysis pupil to determine the maximum defocus change, which was defined as the center of the optical zone. This practice allowed us to obtain centered wavefront error differences independent from potential decentration relative to the real pupil. A custom-programmed MATLAB algorithm (MATLAB 7.2; The MathWorks Inc, Natick, Mass) was used for the simulation of decentration. Decentered wavefront error differences $\Delta W(x', y')$ were calculated for the size of a 6-mm sub-aperture along Cartesian decentrations Δx and Δy, where Δx and Δy were changed in steps of 100 μm covering the entire 9-mm centroid area and resulting in a maximum decentration range of 3000 μm over a circular region. Zernike polynomials for the 2nd to 6th order were fitted to the data of each decentered wavefront, resulting in 709 wavefront errors (1 centered and 708 decentered) per eye. All postoperative wavefront errors were calculated by adding the centered or decentered wavefront error difference value to a standard centered mean wavefront error, which was obtained by averaging the pupil-centered preoperative wavefront errors for the eyes in this study.[19] This practice allowed us to eliminate interindividual differences in preoperative optical quality and internal optics. Therefore, the independent variables in the experiments were the different centered and decentered treatment effects and corresponding changes of the VSOTF[20] image quality metric.

Simulation 1: Optical Quality Of An Uncorrected Eye

This experiment simulated the effects of pupil dilation and optical zone decentration on optical quality of the uncorrected eye relative to a centered PRK correction with no residual refractive error for a 3-mm pupil diameter. This simulation reflects the influence of both LOA and HOA, as induced by decentration and pupil dilation. First, for a centered treatment at a 3-mm pupil diameter, the LOA combination that yielded optimum image quality was determined using Visual Optics Lab-Pro 7.14 (Sarver and Associates, Carbondale, Ill). This program calculated the VSOTF metric and modified LOA coefficients to maximize the VSOTF, simulating the process of subjective refraction. Second, for each decentered position from 0 to 1.5 mm (0.1-mm steps) along the 0°, 90°, 180°, and 270° meridians, pre- to postoperative wavefront error changes were computed. In a third step, wavefront error and VSOTF differences were

recalculated for pupil diameters between 3 and 6 mm in 0.1-mm steps. This procedure generated four x, y, z datasets per eye. A bivariate linear regression model (SPSS 11.0; SPSS Inc, Chicago, Ill) was applied to calculate the simultaneous contribution of pupil dilation and decentration (independent or x and y variables) on the pre- to postoperative change of the log VSOTF (dependent or z variable). The standardized regression coefficients β and the adjusted coefficients of determination R^2 of the four measurements per eye were averaged.

Analysis of decentration tolerance was performed as described elsewhere by calculating the maximum permissible decentration that yielded a critical decrease of VSOTF difference by 0.2 log units.[19] Briefly, vectors $\bar{r}$ between the centered position (x, y) and each outmost coordinate below the criterion (threshold coordinates x′, y′) were calculated. The mean value $\bar{r}$ reflects the average maximum permissible decentration in microns that allows one to remain below the threshold criterion and equals the radius of a circle around the centered position. Tolerance values $\bar{r}$ were calculated based on the entire set of 709 datapoints for pupil diameters between 3 and 6 mm in 0.5-mm steps. A Student *t* test for paired samples was applied to compare decentration tolerance values obtained with different simulation models.

Simulation 2: Uncorrected Optical Quality Relative To A Best-Corrected State At 3-mm Pupil Diameter

In this second simulation experiment, the contribution of decentration and pupil dilation on VSOTF change was simulated for an eye with best correction obtained over a 3-mm pupil diameter. Lower order aberrations were adjusted by VSOTF optimization for each centered or decentered position at a 3-mm pupil diameter. This represents the clinical situation of spectacle correction determined at a 3-mm pupil diameter in an eye with optical zone decentration, ie, possible decentration-induced LOA are compensated for at a 3-mm pupil. Also for this experiment, data analysis steps (regression and decentration tolerance calculation) were performed as described above.

Simulation 3: Best-Corrected Optical Quality

This experimental procedure was similar to those described above; however, for each decentered position and each pupil diameter (ie, each single wavefront error change) the best possible optical quality was calculated using the VSOTF maximization method. Hence, this third experiment assessed the influence of decentration and pupil dilation on HOA induction, as compensation for LOA was made. The further analysis steps (regression and decentration tolerance calculation) were similar to simulation 1.

Statistical Analysis

For comparison between the models, a Student *t* test (after checking normal distribution with a Kolmogorov-Smirnov-Lilliefors test) was applied. If necessary, a Bonferroni correction was performed.

RESULTS

Treatment and wavefront characteristics are summarized in Table 1. In all eyes analyzed, both decentration and pupil dilation led to decreased retinal image quality (VSOTF) relative to the centered, non-dilated state. Figure 1 shows color maps illustrating the simultaneous contribution of pupil dilation and decentration for eye #5-005_OD. For all three simulation models and for all eyes, there was a greater decrease of VSOTF due to pupil dilation than to decentration, which was confirmed by regression analysis (Table 2). For all three simulations, the adjusted R^2 values were high, ranging from 0.94 to 0.96 ($P<.001$), indicating that both pupil dilation and decentration explain most of the variance of the change of retinal image quality (Δ VSOTF) in our model. Analysis of the standardized regression coefficients β showed that

in all three simulation models, pupil dilation had a 2 to 3 times greater influence on Δ VSOTF than decentration (Table 2). The relative influence of decentration was lowest (median β= −0.26) in simulation experiment 2, where decentration-induced LOAs were corrected based on the refraction obtained at a pupil diameter of 3 mm (undilated state). The relative contribution of pupil dilation and decentration was similar in the other models.

Figure 2 shows convolution images simulating the postoperative image quality for three pupil diameters (3, 4.5, and 6 mm) at three horizontal decentration levels (0, 500, and 1500 μm). Figure 2A represents the clinical situation of uncorrected vision of a decentered treatment compared to an outcome with no residual refractive error at the centered position (simulation 1). In this case, image quality is compromised by the induction of both LOAs and HOAs. Figure 2B shows the same situation but with LOAs corrected for a 3-mm pupil diameter at each level of decentration, which represents the situation of an eye with decentered optical zone and LOA correction obtained at a pupil diameter of 3 mm (simulation 2). Comparison of the two convolution simulations shows that correction of decentration-induced LOAs leads to improvement of image quality. The average effect of pupil dilation on Δ VSOTF is illustrated in Figure 3 for decentrations of 0, 500, and 1500 μm, respectively. The graphs that represent the VSOTF changes at the centered and decentered states roughly have a similar shape and run parallel, indicating there is no steeper decrease of Δ VSOTF if the optical zone is decentered.

Decentration tolerance, defined as the maximum permissible decentration that resulted in a VSOTF decline <0.2 log units,[19] decreased with pupil diameter (Table 3, *t*Fig 4). Correction of decentration-induced LOA (3-mm pupil diameter, simulation 2) led to less decrease in VSOTF; which was statistically significant (Student test with Bonferroni correction) for pupil diameters from 3 to 3.5 mm. If LOAs were corrected completely (best-corrected VSOTF, simulation 3), the difference was statistically significant for a 3-, 3.5-, and 5-mm pupil diameter. No statistically significant difference between decentration tolerance values calculated for simulations 2 and 3 was noted (see Fig 4, upper curves), although there was a tendency of less VSOTF decrease if LOA correction was adjusted for all pupil diameters.

DISCUSSION

The present study confirmed the hypothesis that both pupil dilation and decentration contribute to the decrease of retinal image quality after myopic PRK compared to the image quality of a perfectly centered treatment at a 3-mm pupil diameter. This could be expected as the wavefront error increases as a function of pupil diameter[7] and decentration.[19] However, as shown graphically in Figure 1 (0.2 log VSOTF decrease, black dotted line), the influence of pupil dilation prevailed over decentration-induced decreases in image quality. This was confirmed by statistical analysis (Table 2) as standardized regression coefficients β for pupil dilation were at least twice as high as those for optical zone decentration. Moreover, if decentration-induced LOAs were corrected (simulation 2), the influence of decentration further decreased (Table 2, β = −0.26). This suggests that LOAs are primarily responsible for decreases in image quality in the case of decentration. The induction of LOAs by pupil dilation is limited, as reflected by marginal differences between simulation models 2 and 3 (see Figs 3B and 3C). In the latter model, dilation-induced LOAs were corrected. In contrast to similuations 1 and 2, simulation 3 has only theoretical relevance because in clinical practice it is almost impossible to adapt the LOA correction to the actual pupil diameter. The convolution series in Figures 2A and 2B shows the effect of LOA correction in case of pupil dilation and decentration. Figures 1 and 3 also illustrate that in case of micro-decentrations (≤500 μm), the effect on optical quality is rather limited. In particular, we could not support our second hypothesis that micro-decentrations, which are asymptomatic under photopic conditions (in our simulations represented by a 3-mm pupil diameter), become symptomatic under mesopic conditions (6-mm pupil diameter). Only for severe decentrations (eg, 1500 μm) did we observe a somewhat

steeper decrease in retinal image quality with pupil dilation (see Figs 1–3) relative to the centered treatment.

Analysis of decentration tolerance as a function of pupil diameter confirmed results from our previous study[19] and again underlined the role of decentration-induced LOAs (see Fig 4) in lowering retinal image quality. If the strict criterion of a VSOTF decrease of 0.2 log units is applied, the tolerance to decentration at a given pupil diameter was lowest in simulation 1 (LOA no correction, open squares in Figure 4). If decentration-induced LOAs (see Fig 4, gray diamonds) or decentration- and dilation-induced LOAs (see Fig 4, black triangles) were corrected, decentration tolerance increased. This effect was statistically significant, at least for lower pupil diameters.

With regard to clinical practice and as suggested by our previous study,[19] the present simulations showed that ubiquitous optical zone micro-decentrations[10] only have a limited effect on optical quality after laser refractive surgery. However, one should consider that the physiological range of pupil diameters is by far higher than that of our model.[23] In addition, there is more probability that an eye will reach large pupil diameters than high decentration values.[10] This discrepancy of probabilities further decreases the likely influence of decentration on image quality following laser refractive surgery. Even if a relatively strict criterion is applied (as in our decentration tolerance construct), decentrations ~500 μm did not lead to a VSOTF decrease beyond the tolerance threshold (see Fig 4).

Although the present results are in line with clinical experience that micro-decentrations do not inevitably induce optical symptoms, they should be interpreted with some caution. The VSOTF is a theoretical construct, as is the simulation of best-corrected refraction based on the VSOTF. Psychometric tests have shown that subjective quality of vision may differ from the VSOTF.[24] Some patients may be particularly sensitive to decentration-induced coma blur whereas others may exhibit no impairments. Moreover, aberrations induced by optical zone decentration may become more complex in cases of astigmatic or wavefront-guided ablations. Procedures that induce higher amounts of spherical aberration, such as treatments for high myopia[2,25] and hyperopia,[13,25] are also likely to exhibit lower decentration tolerance compared to the treatments investigated in this study.[19] Finally, even this small sample was heterogenous regarding its treatment effects and induced HOA (Table 1). This heterogeneity was also reflected by a relatively large range of decentration tolerance values and regression coefficients. However, a larger sample size is needed to establish any correlation between the amount of attempted correction and the relative contribution of pupil dilation and decentration of optical quality. Regarding comparability of cat with human PRK, analysis of treatment effects showed that the aberration pattern in the cat model is similar to that observed in humans.[14,21] The under-correction on the cat cornea has been observed before and could be explained by a lower ablation rate for the cat cornea.[14,19] Although this heterogeneity of the data somewhat decreased comparability with human data, it does not affect the results from the model itself. Moreover, the cat model is unique as wavefront sensing at a large physiological pupil diameter of 9 mm without pharmacological dilation is possible.[21]

The present model study showed that pupil dilation has a higher impact on the decrease in retinal image quality experienced after myopic PRK than decentration of the ablation optical zone. In particular, for eyes that do not show visual symptoms such as halos and ghosting under photopic conditions but become symptomatic with pupil dilatation, micro-decentrations (≤500 μm) did not induce significant amounts of additional lower or higher order optical aberrations.

Acknowledgments

This study was supported by the Deutsche Forschungsgemeinschaft (DFG) Bu 2163/1-1 (Bühren); the National Institutes of Health (NIH) R01 EY015836 (Huxlin) and Core grant 08P0EY01319F (Center for Visual Science); a

grant from Bausch & Lomb; grants from the University of Rochester Center for Electronic Imaging Systems, a NYSTAR-designated Center for Advanced Technology; and an unrestricted grant from the Research to Prevent Blindness Foundation Inc to the Department of Ophthalmology, University of Rochester.

References

1. Seiler T, Kaemmerer M, Mierdel P, Krinke HE. Ocular optical aberrations after photorefractive keratectomy for myopia and myopic astigmatism. Arch Ophthalmol 2000;118:17–21. [PubMed: 10636408]
2. Moreno-Barriuso E, Lloves JM, Marcos S, Navarro R, Llorente L, Barbero S. Ocular aberrations before and after myopic corneal refractive surgery: LASIK-induced changes measured with laser ray tracing. Invest Ophthalmol Vis Sci 2001;42:1396–1403. [PubMed: 11328757]
3. Kohnen T, Bühren J, Kühne C, Mirshahi A. Wavefront-guided LASIK with the Zyoptix 3.1 system for the correction of myopia and compound myopic astigmatism with 1-year follow-up: clinical outcome and change in higher order aberrations. Ophthalmology 2004;111:2175–2185. [PubMed: 15582071]
4. Bühren J, Kohnen T. Factors affecting the change in lower-order and higher-order aberrations after wavefront-guided laser in situ keratomileusis for myopia with the Zyoptix 3.1 system. J Cataract Refract Surg 2006;32:1166–1174. [PubMed: 16857504]
5. Freedman KA, Brown SA, Mathews SM, Young RS. Pupil size and the ablation zone in laser refractive surgery: considerations based on geometric optics. J Cataract Refract Surg 2003;29:1924–1931. [PubMed: 14604712]
6. Dorronsoro C, Cano D, Merayo-Lloves J, Marcos S. Experiments on PMMA models to predict the impact of corneal refractive surgery on corneal shape. Opt Express 2006;14:6142–6156. [PubMed: 19516786]
7. Bühren J, Kühne C, Kohnen T. Influence of pupil and optical zone diameter on higher-order aberrations after wavefront-guided myopic LASIK. J Cataract Refract Surg 2005;31:2272–2280. [PubMed: 16473217]
8. Mrochen M, Kaemmerer M, Mierdel P, Seiler T. Increased higher-order optical aberrations after laser refractive surgery: a problem of subclinical decentration. J Cataract Refract Surg 2001;27:362–369. [PubMed: 11255046]
9. Porter J, Yoon G, MacRae S, Pan G, Twietmeyer T, Cox IG, Williams DR. Surgeon offsets and dynamic eye movements in laser refractive surgery. J Cataract Refract Surg 2005;31:2058–2066. [PubMed: 16412916]
10. Porter J, Yoon G, Lozano D, Wolfing J, Tumbar R, Macrae S, Cox IG, Williams DR. Aberrations induced in wavefront-guided laser refractive surgery due to shifts between natural and dilated pupil center locations. J Cataract Refract Surg 2006;32:21–32. [PubMed: 16516775]
11. Ou JI, Manche EE. Topographic centration of ablation after LASIK for myopia using the CustomVue VISX S4 excimer laser. J Refract Surg 2007;23:193–197. [PubMed: 17326359]
12. Roberts C. Biomechanics of the cornea and wavefront-guided laser refractive surgery. J Refract Surg 2002;18:S589–S592. [PubMed: 12361163]
13. Yoon G, MacRae S, Williams DR, Cox IG. Causes of spherical aberration induced by laser refractive surgery. J Cataract Refract Surg 2005;31:127–135. [PubMed: 15721705]
14. Nagy LJ, MacRae S, Yoon G, Wyble M, Wang J, Cox I, Huxlin KR. Photorefractive keratectomy in the cat eye: biological and optical outcomes. J Cataract Refract Surg 2007;33:1051–1064. [PubMed: 17531702]
15. Pallikaris I, Kymionis G, Panagopoulou S, Siganos CS, The-odorakis MA, Pallikaris AI. Induced optical aberrations following formation of a laser in situ keratomileusis flap. J Cataract Refract Surg 2002;28:1737–1741. [PubMed: 12388021]
16. Porter J, MacRae S, Yoon G, Roberts C, Cox IG, Williams DR. Separate effects of the microkeratome incision and laser ablation on the eye's wave aberration. Am J Ophthalmol 2003;136:327–337. [PubMed: 12888057]
17. Potgieter FJ, Roberts C, Cox IG, Mahmoud AM, Herderick EE, Roetz M, Steenkamp W. Prediction of flap response. J Cataract Refract Surg 2005;31:106–114. [PubMed: 15721702]

18. Netto MV, Wilson SE. Corneal wound healing relevance to wavefront guided laser treatments. Ophthalmol Clin North Am 2004;17:225–231. vii. [PubMed: 15207564]

19. Bühren J, Yoon G, Kenner S, MacRae S, Huxlin K. The effect of optical zone decentration on lower- and higher-order aberrations after photorefractive keratectomy in a cat model. Invest Ophthalmol Vis Sci 2007;48:5806–5814. [PubMed: 18055835]

20. Cheng X, Thibos LN, Bradley A. Estimating visual quality from wavefront aberration measurements. J Refract Surg 2003;19:S579–S584. [PubMed: 14518747]

21. Huxlin KR, Yoon G, Nagy L, Porter J, Williams D. Monochromatic ocular wavefront aberrations in the awake-behaving cat. Vision Res 2004;44:2159–2169. [PubMed: 15183683]

22. Thibos LN, Applegate RA, Schwiegerling JT, Webb R. VSIA Standards Taskforce Members. Vision science and its applications. Standards for reporting the optical aberrations of eyes. J Refract Surg 2002;18:S652–S660. [PubMed: 12361175]

23. Rosen ES, Gore CL, Taylor D, Chitkara D, Howes F, Kowalewski E. Use of a digital infrared pupillometer to assess patient suitability for refractive surgery. J Cataract Refract Surg 2002;28:1433–1438. [PubMed: 12160815]

24. Bühren J, Strenger A, Martin T, Kohnen T. Wavefront aberrations and subjective quality of vision after wavefront-guided LASIK: first results [German]. Ophthalmologe 2007;104:688–696. [PubMed: 17551732]

25. Kohnen T, Bühren J. Corneal first-surface aberration analysis of the biomechanical effects of astigmatic keratotomy and a micro-keratome cut after penetrating keratoplasty. J Cataract Refract Surg 2005;31:185–189. [PubMed: 15721711]

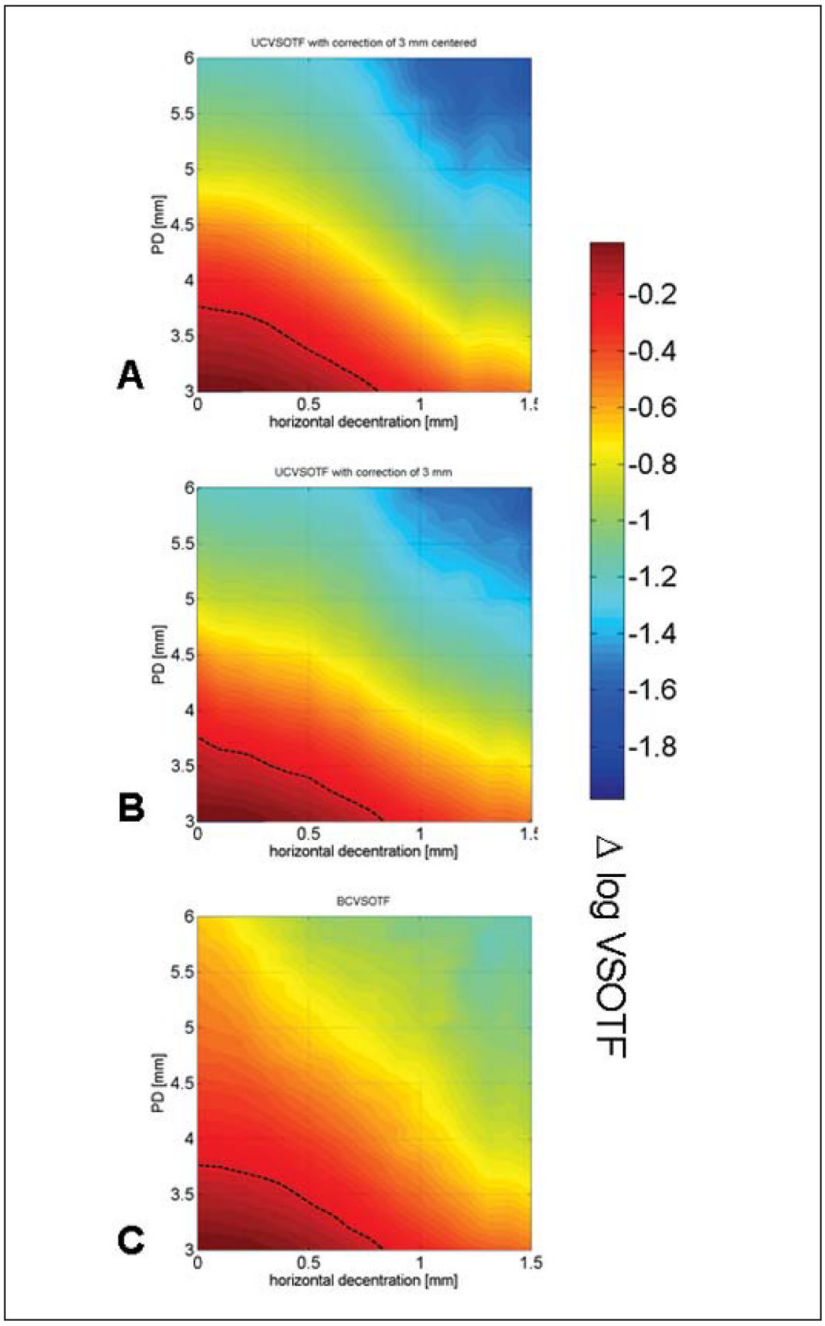

Figure 1.

Color maps showing the simultaneous effect of decentration and pupil diameter (PD) on the change of retinal image quality (visual Strehl ratio based on the optical transfer function [Δ log VSOTF]) for eye #5-005_OD. **A)** Simulation 1: optimum lower order aberration (LOA) correction obtained at a 3-mm pupil diameter; no correction of LOA for any decentered position or dilated pupil. **B)** Simulation 2: optimum LOA correction obtained at a 3-mm pupil diameter for any decentered position; no adjustment for any dilated pupil. **C)** Simulation 3: optimum LOA correction at all decentered positions and adjustment for all pupil dilations. Dotted line = 0.2 log VSOTF decrease threshold

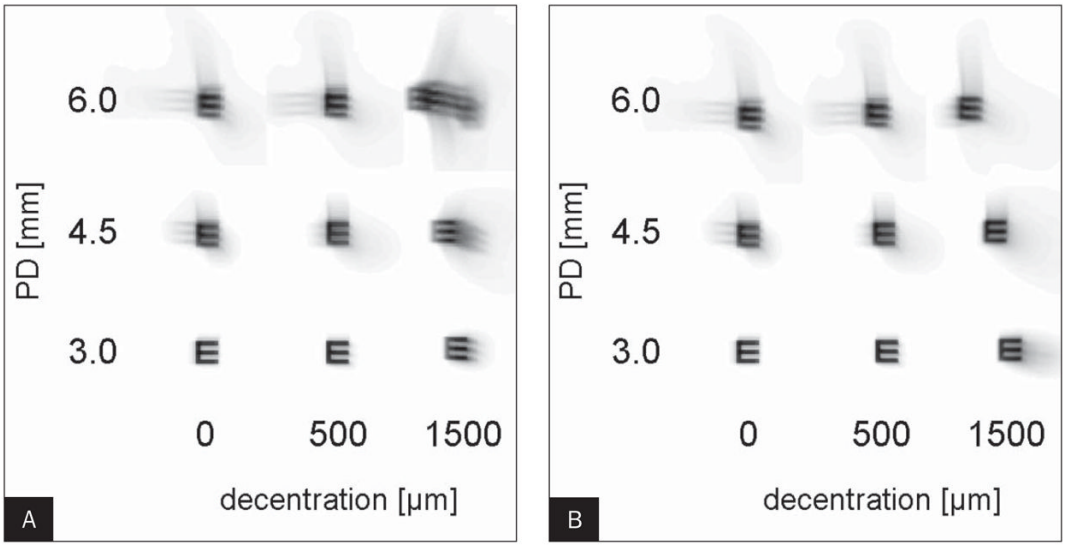

Figure 2.

Image simulation of postoperative image quality by convolution for eye #5-005_OD. The convolution images are not corrected for phase shift. **A)** Simulation 1: optimum lower order aberration (LOA) correction obtained at a 3-mm pupil diameter (PD); no correction of LOA for any decentered position or dilated pupil. **B)** Simulation 2: optimum LOA correction obtained at a 3-mm pupil diameter for any decentered position; no adjustment for any dilated pupil.

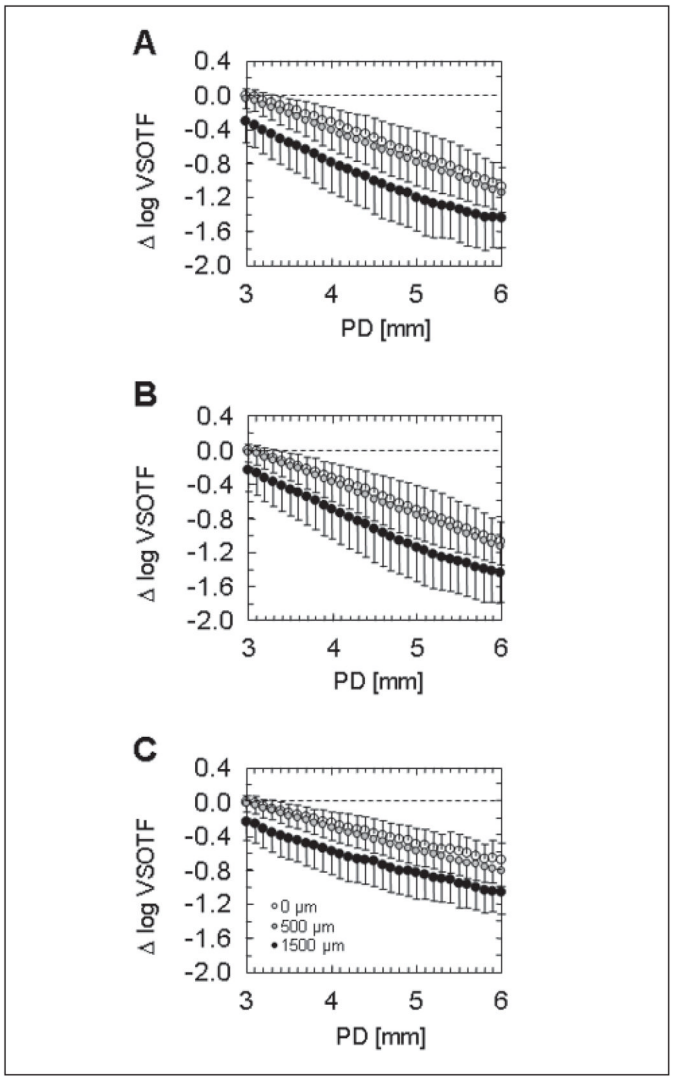

Figure 3.

Comparison of change of visual Strehl ratio based on the optical transfer function (Δ VSOTF) as a function of pupil diameter (PD) for three grades of decentration (0, 500, and 1500 μm); average values from all five eyes. The centered value obtained for a 3-mm pupil diameter is set to zero. **A)** Simulation 1: optimum lower order aberration (LOA) correction obtained at a 3-mm pupil diameter; no correction of LOA for any decentered position or dilated pupil. **B)** Simulation 2: optimum LOA correction obtained at a 3-mm pupil diameter for any decentered position; no adjustment for any dilated pupil. **C)** Simulation 3: optimum LOA correction at all decentered positions and adjustment for all pupil dilations.

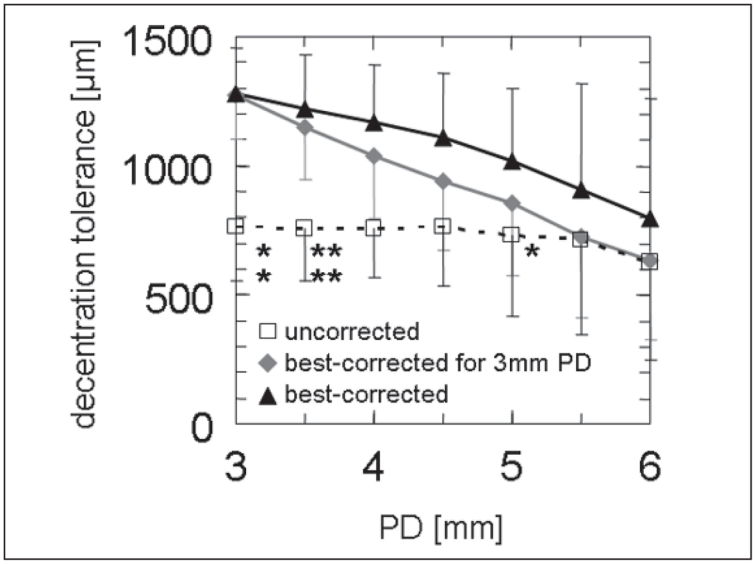

Figure 4.

Comparison of decentration tolerance (maximum permissible decentration to maintain a decrease of visual Strehl ratio based on the optical transfer function [VSOTF] of <0.2 log units). The asterisks denote significance of difference between correction modes (*P<.05, **P<.01 after Bonferroni correction). Asterisks, top row: difference between uncorrected and best spectacle-corrected mode; bottom row: difference between uncorrected and best spectacle-corrected at 3-mm mode. Differences between best-corrected and best-corrected at 3-mm mode did not reach statistical significance.

TABLE 1

Treatment Characteristics and Wavefront Error Changes for the Centered Treatment Over 6-mm Pupil Diameter

				Centered Wavefront Error Change Δ W(x, y)						
Eye	**Treatment(D)**	**OZ (mm)**	**TTZ (mm)**	**Sphere(D)**	**Cylinder(D)**	**Axis (°)**	**Total HOA RMS (μm)**	**Coma RMS (μm)**	**SA RMS(μm)**	**rHOA RMS (μm)**
c1-005 OD	−6. 00	8	11.1	+4.71	−0.61	12	0.541	0.197	0.333	0.388
c2-001 OS	−6.00	6	9.1	+2.17	−0.65	88	0.618	0.285	0.327	0.440
c2-006 OS	−6.00	6	9.1	+2.56	−0.24	40	0.307	0.120	0.039	0.280
c5-005 OD	−10.00	6	9.1	+4.11	−0.28	37	0.574	0.296	0.426	0.246
c5-026 OD	−10.00	6	9.1	+5.29	−0.47	160	0.430	0.291	0.262	0.178

OZ = diameter of the programmed optical zone, TTZ = diameter of the total treatment zone, Total HOA RMS = root-mean-square value of 3rd to 10th order aberrations, Coma RMS = RMS value of 3rd to 9th order coma, SA RMS = RMS value of 4th to 10th order spherical aberration, rHOA RMS = residual RMS of all non-coma, non-spherical HOAs, OD = right eye, OS = left eye

J Refract Surg. Author manuscript; available in PMC 2010 March 18.

TABLE 2

Regression Analysis of the Influence of Pupil Diameter and Decentration on Postoperative Image Quality (log VSOTF)

Simulation	R^2 (Adjusted)	Predictor	Standardized Regression Coefficients β
(1) Uncorrected with optimum refraction for a 3-mm pupil diameter at centered position	0.94 (0.87 to 0.98)	Pupil diameter	−0.88 (−0.99 to −0.67)
		Decentration	−0.45 (−0.67 to 0.23)
(2) Uncorrected with optimum refraction for a 3-mm pupil diameter	0.96 (0.88 to 0.96)	Pupil diameter	−0.95 (−0.99 to −0.80)
		Decentration	−0.26 (−0.49 to 0.23)
(3) Best-corrected	0.95 (0.88 to 0.97)	Pupil diameter	−0.87 (−0.98 to −0.73)
		Decentration	−0.42 (−0.64 to 0.11)

Note. The table shows the median, minimum, and maximum of the coefficients of determination (R^2) and standardized regression coefficients (β). All correlations were statistically significant (P<.001).

TABLE 3

Analysis of Decentration Tolerance* for 3- and 6-mm Pupil Diameters

	$\bar{r}$ (μm)	
Simulation	**3-mm PD**	**6-mm PD**
(1) Uncorrected with optimum refraction for 3-mm PD at centered position	766±211	624±378
(2) Uncorrected with optimumn refraction for 3-mm PD	1219±210	633±308
(3) Best-corrected	1279±175	797±461

PD = pupil diameter

* Maximum permissible decentration to maintain a decrease of VSOTF<0.2 log units.

Note. The radius $\bar{r}$ is the mean length of the vectors between the center and the locations with threshold values.